Nutrient content controls onset of lignin decomposition in Beech litter

Lukas Kohl[1], Wolfgang Wanek[1], Katharina Keiblinger[2,3], Sonja Leitner[1,3], Maria Mooshammer[1], Ieda Hämmerle[1], Lucia Fuchslueger[1], Jörg Schnecker[1], Thomas Schneider[4,5] Sandra Moll[7] Markus Gorfer[7,8] Joseph Strauss[7,8] Katharina Riedel[4,6] Leo Eberl[4,5] Sophie Zechmeister-Boltenstern[2,3], Andreas Richter[1],

1 Department of Chemical Ecology and Ecosystem Research, University of Vienna, Althanstrasse 14, A-1090 Vienna, Austria

2 Federal Research and Training Centre for Forests, Natural Hazards and Landscape, Department of Soil Biology, Seckendorff-Gudent-Weg 8, A-1131 Vienna, Austria

3 Current address: Institute for Soil Science, University of Natural Resources and Life Sciences, Peter Jordan-Straße 82, A-1180, Vienna, Austria

4 Institute of Plant Biology, University of Zurich, Winterthurerstrasse 190, CH-8057, Zurich, Switzerland

5 Current address: Institute of Plant Biology, University of Zurich, Zollikerstrasse 107, CH-8008, Zurich, Switzerland

6 Current address: Institute of Microbiology, Ernst-Moritz-Arndt University of Greifswald, Friedrich-Ludwig-Jahn-Strasse 15, D-17487 Greifswald, Germany

7 Fungal Genetics and Genomics Unit, Department of Applied Genetics and Cell Biology, University of Natural Resources and Life Sciences, Konrad-Lorenz-Strasse 24, A-3430 Tulln, Austria

8 AIT Austrian Institute of Technology GmbH, Bioresources Unit, Konrad-Lorenz-Strasse 24, A-3430 Tulln, Austria

∗ **E-mail: Corresponding author@institute.edu**

Abstract

Lignin is a major component of plant litter and is considered highly resistant to decomposition. Polymeric carbohydrates, in contrast, are more easily accessible carbon sources. We studied the decomposition rates of these two compound classes, to which extent they are controlled by litter C:N:P stoichiometry, and whether this control changes over time. Therefore, we conducted a 15-months mesocosm experiment under controlled climatic conditions, comparing beech litter of different N and P contents, which was sterilized and re-inoculated with a litter/topsoil mixture from one of the sites to ensure identical microbial communities at the start of the experiment. Lignin and carbohydrate decomposition rates were calculated for 2 periods (0-6 months and 6-15 months) by pyrolysis-GC/MS.

Positive correlations of carbohydrate decomposition rates with litter N content were found during the entire experiment. Lignin decomposition rates during the initial period were highly variable and negatively correlated to litter P content and positively correlated to the microbial P demand ($C:P_{litter}/C:P_{microbial}$). During the later stage, both lignin and carbohydrate decomposition loss were positively correlated to N contents and respiration. Initial lignin decomposition rates were highest in litter with low fungi:bacteria ratios, which occurred in N and P poor litter.

Our results showed that a substantial amount of lignin can be degraded during early decomposition. In the present study, early lignin decomposition was coupled to low N and P availability, and the establishment of K-strategist microorganisms. However, early lignin decomposition rates did not depend on fungi, which are commonly assumed to mediate lignin decomposition, or stoichiometric conditions that favor fungal growth.

Introduction

Plant litter is quantitatively dominated by macromolecular compounds. In foliar litter, lignin and carbohydrate polymers together make up 40-60% of litter dry mass [1], while leachable substances ("DOM") account for only 1.5-6% [2]. The breakdown of these high molecular weight compounds into smaller molecules accessible to microbes is mediated by extracellular enzymes and is therefore considered to be the rate limiting for decomposition processes [3]

Common models of litter decomposition [4–7] assume that organic compounds in litter form up to three independent pools of increasing recalcitrance, i.e. (1) soluble compounds, (2) cellulose and hemi-celluloses, and (3) lignin and waxes (cutin and suberin). Soluble compounds are most accessible to microbes and are usually consumed first, followed by regular polymers, such as cellulose. Lignin is not degraded until accumulated to a certain, critical level when it inhibits the degradation of less recalcitrant compounds. Most studies quantified these pools by gravimetric determination of the amount of cellulose, hemi-celluloses and lignins after sequential extractions with selective solvents. These methods were repeatedly criticized for being unspecific for lignin determination [8]. When analyzed with alternative methods (NMR, CuO-oxidation, Pyrolysis-GC/MS), extracted lignin fractions were shown to contain also many other substances [9].

Recent studies based on more specific methods to determine litter lignin contents question the intrinsic recalcitrance of lignin. Isotope labeling experiments with soils and litter/soil mixtures, undertaken both in-situ and under controlled conditions, revealed mean residence times of lignin in soils in the range of 10-50 years, much less then expected and shorter than that of bulk soil organic matter [10–12]. While the ability to completely degrade lignin was traditionally attributed exclusively to Basidomycetes, it has been demonstrated for several bacterial taxa over the last years [13].

For leaf litter, lignin decomposition even at early stages of litter decay and lignin decomposition rates that decreased during decomposition were recently reported by Klotzbücher and colleagues [14]. Based on these results, they proposed a new concept for lignin degradation in which fastest lignin degradation occurs during early litter decomposition when the availability of labile carbon sources is high. Lignin decomposition during late decomposition, in contrast, is limited by the availability of easily assimilated C and therefore slows down. Additionally, the decomposition of lignin may also be dependent on the nutrient content of the litter and thus the nutritional status of the microbial community. During radical polymerization, significant amounts of cellulose and protein are incorporated into lignin structures [15]. In isolated lignin fractions from fresh beech litter, N contents twice as high as in bulk litter were found [16]. It was therefore argued

that, while yielding little C and energy, lignin decomposition makes protein accessible to decomposers that is occluded in plant cell walls, and that lignin decomposition is therefore not driven by C but by the N demand of the microbial community ("Nitrogen mining theory", [17]).

In favor of the N mining theory, fertilization experiments indicated N exerts an important control on lignin degradation: N addition increased mass loss rates in low-lignin litter while slowing down decomposition in lignin-rich litter [18] and decreased the activity of lignolytic enzymes in forest soils [3]. Moreover, cellulose triggered a stronger priming effect in fertilized than in unfertilized soils indicating that the mineralization of recalcitrant carbon may be controlled by an interaction of N and labile C availability [19].

Addition of N has a different effect on litter decomposition than varying N levels in the litter [20]. This is due to the fact that leaf litter N is stored in protein and lignin structures and not directly available to microorganisms, while fertilizer N is added in the form of readily available inorganic N (ammonium, nitrate or urea). N-fertilization experiments can thus simulate increased N-deposition rates but not the effect of litter N on decomposition processes.

Our study therefore aimed at analyzing the effect of variations in beech litter nutrient (N and P) content and stoichiometry (C:N and N:P ratios) on lignin and carbohydrate decomposition rates. Towards this end, we followed the breakdown of lignin and polymeric carbohydrates by pyrolysis-GC/MS (pyr-GC/MS) during a mesocosm experiment under constant environmental conditions over a period of 15 month. In order to exclude effects resulting from different initial microbial communities, we sterilized beech litter samples from 4 different locations in Austria and re-inoculated them prior to the experiment with an litter/top-soil inoculum from one of the sites. Additionally, we analyzed the micorbial community in a subset of the samples using a metaproteomic approach.

With the experiment, we addressed the following questions:

(Q1) Is lignin decomposition delayed until late decomposition stages or are significant amounts of lignin already degraded during early litter decomposition, and is the timing of lignin decomposition dependent on litter stoichiometry? We hypothesized, that ligin decomposition is initially slower in litter with a narrow C:N ratio (higher availability of assimilable nitrogen), than in litter with a high C:N ratio.

(Q2) Are high lignin degradation rates related to a higher fungal activity? We hypothesized that wider C:N and C:P ratios favor lignin degradation by fungi while narrow C:N and C:P ratios favor carbohydrate degradation by bacteria.

Results

Initial litter chemistry

Initial litter chemistry of the four sites (Achenkirch, AK, Klausenleopoldsdorf, KL, Ossiach, OS, Schottenwald, SW), measured 14 days after incubation, is presented in supplemental table 1. C:N ratios varied between 41:1 and 58:1 and C:P ratios between 700:1 and 1300:1, while N:P ratios ranged between 15:1 and 30:1. No significant changes occurred during litter incubation except a slight decrease of the C:N ratio (41.8:1 to 37.4:1) found in the most active litter type (SW) after 15 months. Fe concentrations were more than twice as high for OS (approx. 450 ppm) than for other litter types (approx. 200 ppm). Litter Mn also was highly variable between litter types, ranging between 170 and 2130 ppm. Changes of micro-nutrient concentrations during litter incubation were significant, but in all cases <15% of the initial concentration. In initial litter, lignin accounted for 28.9-31.2% and carbohydrates for 25.9-29.2% of the total peak area of all pyrolysis products.

Mass loss, respiration and soluble organic carbon

Litter mass loss was not significant after 2 weeks and 3 months, and significant for 2 litter from two sites after 6 months. After 15 months, litter mass loss was significant for all collection sites, and ranged between 5 and 12 % of the initial dry mass, and was strongly correlated to litter N content ($R=0.794$, $p<0.001$). Detailed results were reported by [21].

Highest respiration rates were measured at the first measurement after 14 days incubation (150-350 µg CO_2-C d^{-1} g^{-1} litter-C), which dropped to 75 to 100 µg CO_2-C d^{-1} g^{-1} litter-C after 3 months. After 6 and 15 months, respiration rates for AK and OS further decreased, while SW and KL showed a second maximum in respiration after 6 months (fig 1). Accumulated respiration was strongly correlated to litter mass loss after 15 months ($r=0.738$, $p<0.001$, $n=20$).

Soluble organic carbon concentrations decreased between the first three harvests (14 days to 6 months), and strongly increased to 15 months (from 0.1 to 0.7 mg C g^{-1} d.w. to 1.5 to 4 mg C g^{-1} d.w. after 15 months, fig. 1). After 14 days and 3 months, the highest soluble organic C concentrations were found in SW litter followed by AK. Soluble organic C concentrations were weakly correlated with litter N content after 14 days ($r=0.69$, $p<0.001$, $n=20$) and after 3 months ($r = 0.65$, $p<0.01$, $n=20$), but strictly correlated after 6 months ($r=0.85$, $p<0.001$, $n=20$) and 15 months ($r=0.90$, $p<0.001$, $n=20$).

Potential enzyme activities

Within each time point, all potential extracellular enzyme activities were correlated with litter N and actual respiration rates(all $R>0.8$, $p<0.001$, $n=20$). Cellulase activity increased from the first harvest onwards to 15 months, with a small depression after 6 months (Fig. 1), phenoloxidase and peroxidase activities reached their maximum between 3 and 6 months (fig. 1). For all enzymes and at all time points, SW showed the highest and AK the lowest activities. Differences between these two sites were more pronounced in cellulase activity (SW 10x higher than AK) than in oxidative enzymes (SW 4x higher). Conversely, the phenoloxidase/cellulase ratio was highest for AK and lowest for SW at all time points and decreased during litter decomposition (fig. 1).

Microbial biomass abundance and community composition

Microbial biomass contents ranged from 0.5 to 6 mg C g^{-1} d.w., 0.05 to 0.55 mg N g^{-1} d.w. and 0.05 to 0.35 mg P g^{-1} litter d.w (fig. 2). After an initial increase in microbial biomass, in KL and OS microbial biomass remained constant after 3 months while AK and SW showed further accumulation of microbial biomass which reaches a maximum of microbial C and N contents after 6 months (AK also for P). Microbial C:N ratios ranged between 6:1 and 18:1, C:P ratios between 8:1 and 35:1, and N:P ratios between 0.5:1 and 3.5:1 (fig. 2).

Microbial biomass was stoichiometrically homeostatic during the first 6 months (no or negative correlations between microbial C:N:P and litter C:N:P, see also [21]), but after 15 months (microbial C:N:P ratios were significantly and positively correlated to resource stoichiometry: R=0.53-0.64, all $p<0.002$). The homeostatic regulation coefficients [22] were $H_{C:P}=1.68$, $H_{C:N}=2.01$, and $H_{N:P}=2.29$ after 15 month incubation. Microbial C:N ratios after 3 and 6 months were within a tighly constrained range, 14.5:1 to 18.2:1 after 3 months and 6.9:1 to 9.0:1 after 6 months, but significantly different between the two sampling events. In contrast, microbial C:P and N:P ratios were less constrained, with the highest variance between litter from different sites after 3 months of incubation (fig. 2).

Metaproteome analysis yielded between 451 and 1113 (average 639) assigned spectra per sample (one replicate per collection site after 14 days, 3, 6, and 15 months). For community profiling only spectra assigned to bacteria or fungi were used. Fungal proteins were dominant in all litter types at all stages, but most prominent in SW and least pronounced in AK. Fungi:bacteria (F:B) protein abundance ratios were highest after 14 days (5 to 12) and decreased during litter decomposition (1.7 to 3 after 15 months, see fig. 4).

The large initial differences in F:B ratios between litter from different sites decreased during decomposition. In addition, F:B ratios were measured on a DNA basis (qPCR) the results showing a similar pattern but with a much larger fungal DNA dominance (F:B ratios between 10-180). F:B ratios were highly correlated between protein- and log-transformed DNA-based estimates ($r=0.785$, $p<0.001$, $n=20$).

Fungal communities were dominated by Ascomycota, with smaller contributions by Basidiomycota (<5% of fungal protein). Among the fungal classes found, Sordariomycetes and Eurotiomycetes were most abundant with further contributions of Dothideomycetes, Leothiomycetes and Saccharomycetes (fig. 3). Bacteria were dominated by Proteobacteria (mainly γ, declining, and α- and β-Proteobacteria, increasing with litter decomposition) with minor contribution of Actinomycetes and Bacterioidetes (both increasing) and Thermotogae (decreasing, fig. 3).

Pyrolysis-GC/MS and Lignin content

In total 128 pyrolysis products were detected, quantified, identified and assigned to their substances of origin (suppl. tab. 2 -4). We found only minor changes in the relative concentration of litter pyrolysis products during decomposition, and differences between sites were small but well preserved during decomposition. However, the high precision and reproducibility of pyrolysis GC/MS analysis of litter allowed tracing small changes in lignin and carbohydrate abundance during decomposition. Lignin-derived compounds made up between 29 and 31 % relative peak area (TIC) in initial litter, and increased by up to 3 %. The increase occured almost exclusively during the first 6 months. Carbohydrate-derived pyrolysis products accounted for 26 to 29 % in initial litter and decreased by up to 2.6 % within 15 months of incubation. The initial (pyrolysis-based) lignin:carbohydrate indices (LCI) were highly similar between litter from different collection sites, ranging between 0.517 and 0.533 (Fig. 4). During decomposition, the LCI increased by up to 9 % of the initial value. The highest increase was found in SW litter, while LCI slightly decreased in AK litter. All significant changes in LCI occurred within the first 6 months (fig. 5). As differences in lignin and carbohydrate contents between 0-3 and 3-6 months were not significant, we analyzed differences for two time intervals, i.e. between 0-6 months and 6-15 months.

During the first 6 months, between one and 6 % of the initial lignin pool and between 4 and 17% of the initial carbohydrate pool were degraded (Fig. 6). Lignin decomposition was highest in AK and KL litter, while microbial communities of KL, OS and SW litter decomposed carbohydrates faster. Lignin preference values (% lignin decomposed : %carbohydrates decomposed) were lowest in SW and highest in AK litter (Figure 5). In AK litter, lignin macromolecules were 50 % more likely to be decomposed than carbohydrates,

while in SW litter carbohydrates were 10 times more likely to be decomposed (fig. 6). Between 6 and 15 months, no further accumulation of lignin occurred. Lignin and carbohydrates were both degraded at the same rate and their relative concentrations remained constant between 6 and 15 months (fig. 6).

Correlations between lignin and carbohydrate decomposition and litter chemistry, microbial community and decomposition processes

Relationships between lignin and carbohydrate degradation, litter chemistry, microbial biomass and decomposition processes were tested after 6 and 15 months (tables **??** and **??**) including data presented by [21] and [23]. After 6 months, we found that the ratio of lignin/cellulose degradation was positively correlated with the ratio of phenoloxidase : cellulase ($R=0.599$, $p=0.005$, $n=20$) and peroxidase : cellulase ($R=0.734$ $p<0.001$, $n=20$). Carbohydrate decomposition was positively correlated with litter N content, and negatively with litter C:N ratios and litter-microbial C:N imbalances. In contrast, lignin decomposition was negatively correlated to litter P, but positively with litter C:P and N:P ratios, and litter-microbial C:P and N:P imbalances (fig. 7). After 15 months, the ratio of lignin : carbohydrate decomposition was no longer related to stoichiometry or elemental composition any more. Most interestingly, lignin and carbohydrate decomposition exhibited the same controls, being positively correlated to soluble organic C, litter N and litter P (table **??**) between 6 and 15 months. Mass loss and accumulated respiration were positively correlated to lignin and carbohydrate decomposition (table **??**), a pattern that we did not find for lignin decomposition in the early decomposition phase (table **??**). Protein abundance F:B ratios were negatively correlated to the ratios of lignin : cellulose decomposition and to LCI change during the first 6 months, pointing to bacterial engagement in lignin decomposition. In contrast, both lignin and carbohydrate decomposition rates, were positively correlated with F:B ratios after 15 months, pointing to fungal dominance of both lignin and carbohydrate decompostion. No correlation between F:B ratio and the ratio of lignin : cellulose decomposition was found in this later period (fig. 4).

To asses the interaction between litter chemistry, microbial community and degradation processes, we conducted a correspondence analysis (CA) of the metaprotomen data (relative protein abundances, fig. 8). The results indicate that incubation time (i.e. succession) is the dominant factor controlling the microbial community, with samples collected at the first (14 days) and the last (15 month) sampling grouping closely together, while litter quality (i.e. elemental stoichiometry of litter collected at different sites) had a higher impact after 3 and 6 months. The first factor (CA 1), which explained 35.7 % of the total variance, separates

litter sampled after 15 months (positive values) from litter sampled earlier (negative values). Consequently, CA 1 was also positively correlated to incubation time and negatively to litter C content (i.e. decreasing C:N ratios during decomposition). A number of bacterial taxa (Actinobacteri, Bacteroidetes, α- and β-proteobacteria), and two fungal classes (Leotiomycetes and Tremellomycetes) were positively correlated to CA1 i.e. increased in abundance towards 15 months, while Cyanobacteria, ϵ-proteobacteria and Saccharomycetes were negatively correlated. CA 2, which explained 26.0 % variance, separated litter sampled within the first 6 months. Dothideomycetes and Sordariomycetes were positively and γ-proteobacteria negatively correlated to this factor, which also correlated to the F:B protein abundance ratio. Litter collected 14 days after inoculation have the highest scores on CA 2, while sites with active lignin degradation within the first 6 months (AK, KL) have the most negative scores. The axis was furthermore correlated to the microbial biomass P content and C:P and N:P imbalances (and free NH_4^+, not shown). For samples analyzed after 6 months, where direct comparison to lignin degradation rates was possible, significant correlations to CA 2 were found for lignin : carbohydrate degradation (r=-0.97, p=0.028), % Lignin loss : % Carbon loss (r=-0.96, p=0.040) and LCI increase (r=0.973, p=0.027), even though the number of independent samples was very low (n=4). Differences in CA2 strongly decreased after 15 months, suggesting that the differences in the microbial community found within the first 6 months were diminished with succession of the decomposer community. Litter N and P contents were not correlated to either factor, although differences in resource quality evidently affected community composition after 3 and 6 months, as can be seen in the differences in the microbial communities as observed in CA 2. Correlation of CA factors with litter stoichiometry, and microbial stoichiometry, and the abundance of the analyzed taxa are provided in supplemental table **??**.

Discussion

The experimental approach chosen allowed us to single out the effects of litter quality on the microbial decomposer community and decomposition processes, while excluding effects of fauna, climate and different initial microbial communities. By exploiting intra-specific differences in beech litter stoichiometry, we were able to minimize differences in the chemical composition of initial litter (e.g. similar lignin and cellulose content, table 1), while exploring the effect of litter nutrient contents on lignin and carbohydrate decomposition. Therefore, we can attribute different rates of carbohydrate and lignin decomposition to the intrinsic qualities of litter collected at different sites, i.e. elemental and stoichiometric composition. Analytical pyrolysis allowed specific determination of litter lignin contents (simultaneously with carbohydrates), avoiding

the limitations of common methods for lignin quantification as AUR [8].

Contradicting traditional concepts of litter decomposition, our results demonstrate that variable amounts of lignin were degraded during the first 6 months of incubation. During this early stage, lignin decomposition rates depended on litter quality (P) and ranged from non-significant to degradation rates similar to bulk carbon mineralization rates (i.e. no discrimination against lignin). Our study therefore provided evidence that early lignin decomposition rates are by far underestimated, as recently proposed by Klotzbücher and coworkers [14], based on a complementary analytic approach. Unlike them, we found no decrease but constant or increasing lignin decomposition rates during litter decomposition over 15 months.

Our results provide strong evidence that litter C:N:P stoichiometry and litter element concentrations exerted a major control on the extent of lignin decomposition during the initial decomposition phase. Carbohydrate decomposition was positively correlated with litter N contents and negatively to litter C:N ratios, as were the majority of decomposition processes (mass loss, respiration, potential extracellular enzymatic activities). In contrast, lignin decomposition rates were positively correlated with litter C:P ratios and negatively with dissolved and total litter P. The relationship was strongest when lignin decomposition rates were compared to litter-microbe C:P imbalances, i.e. the greater the imbalance between resource and consumer C:P (greater P limitation), the lower the lignin decomposition rates. Additionally, we found a marked change in the controls of lignin decomposition during this period. While carbohydrate and lignin decomposition were differently controlled by litter chemistry (N versus P) during the first 6 months, these litter components were decomposed at similar rates thereafter and decomposition rates were only related to litter N availability.

Cultivation studies showed that lignin decomposition by fungi is triggered by N starvation, and that lignin does not provide sufficient energy to maintain the decomposer's metabolism without the use of other organic C i.e. energy sources [24]. Moreover, lignin decomposition was found in wild-type *A. thaliana* litter containing abundant cellulose as a C source, but not in a low-cellulose mutant during a 12-month incubation experiment in a boreal forest [20]. In the N- and P-(co-)limited situation commonly encountered during early litter decomposition, we may speculate that lignin is degraded to access additional nutrients (mainly N) or to use a C surplus by decomposing a less C efficient but nutrient enriched substrate (nutrient mining hypothesis). However, a stimulation of lignin decomposition by low P availability or microbial P limitation, as indicated by the strong negative correlations to P pools that we found, has not been reported yet. Though lignified materials have been reported to be N-rich and decomposition of these materials may therefore enhance N supply to microbial communities, lignins are not expected to contain quantitative important amounts of P.

In order to decompose litter lignin and carbohydrates, microbial decomposers rely on the production and

excretion of hydrolytic and oxidative extracellular enzymes. While the absolute amounts, in which these enzymes are produced, were largely controlled by N availability, the ratio in which they were produced was strongly related to differences in the ratio of cellulose:lignin decomposition. Talbot and coworkers [20] recently suggested that lignin decomposition comprises a strategy of slow-growing microbes to evade competition through colonizing more lignin-rich and nutrient-poor substrates. Indeed we found lignin decomposition in low quality litter (low N and P) with microbial communities that were subject to large imbalances in C:N and C:P between resource and consumer, pointing to N or P limitation. Low P availability may limit fast growth of microbial populations and select for slow-growing lignin-degrading microbes during early decomposition and provide K-strategists (slow growing on recalcitrant carbon) an advantage over r strategists (fast growing on labile carbon). Indeed we found that lignin decomposition was highest in AK litter, where resource C:P and N:P were highest, i.e. low P supply may have limited microbial growth generally or the establishment of r strategists in particular.

Differences in initial lignin contents were marginal (29-31 % relative peak area), and lignin degradation rates of sites with high lignin contents were not higher than that of sites with low lignin contents. Therefore, in early lignin decomposition was not triggered by critical lignin contents (i.e. lignin limiting the use of other C sources) as is suggested by traditional litter decomposition models. Neither did low lignin decomposition rates result from a lack of metal cofactors of oxidative lignin decay (i.e. Mn or Fe), which were suggested to be rate limiting for late lignin decomposition [1]. While Mn and Fe concentrations indeed strongly varied between litter collected at different sites, concentrations were lowest in the litter with highest lignin decomposition rates (AK, see Table 1). Moreover, soluble organic C ("DOC") was suggested to limiting lignin decomposition since the process of lignin decomposition does not generate sufficient energy to power the metabolism of its decomposers [14]. However, soluble organic C did not control lignin decomposition in this experiment since we found highest (initial) concentrations in the two litter types that showed the highest and the lowest lignin decomposition rates (SW and AK). In contrast, while the initial content of soluble C is not related to litter stoichiometry or respiration, we found a strong correlation of soluble C, litter N after 6 and 15 months. This rather supports a perspective in which soluble C is rapidly used by litter decomposers, while its production is limited by the production of extracellular enzymes and therefore by N availability, which in our experiment also correlated with overall C mineralization rates.

While the mode of negative P regulation on lignin decomposition remains unknown, we found corresponding differences in the composition of the microbial decomposer communities on litter with fast and slow lignin decomposition. Unlike predicted by ecological stoichiometry theory, not bacteria but fungi were

more successful in colonizing high N and P litter during initial decomposition. Fungi colonized litter faster than bacteria and therefore dominated early litter decomposition, however the F:B ratios decreased over the entire incubation period pointing to increasing population sizes of bacteria with time. Interestingly, low F:B communities (AK) were more active in decomposing lignin than those being dominated by fungi. This does not necessarily indicate that bacteria play the key role in lignin decomposition, though bacteria were also reported to produce oxidative enzymes that can decompose lignified materials in litter [13]. However, decreases in F:B ratios may be superimposed on the increase of smaller subpopulations of e.g. fungi that are key mediators of lignin decomposition, or alternatively general increases in the size of microbial communities with declining fungi/bacteria ratios may as well mask stable fungal populations when bacterial abundance increases. Furthermore, we are well aware of the short-coming of metaproteomic approaches that under-represent important soil phyla such as uncultivated and unsequenced groups (e.g. Lecanoromycetes).

The onset of lignin degradation in litter from all sites between 15 months was accompanied by increased abundance of fungal and bacterial taxa associated with late litter decomposition: Complete lignin degradation is most commonly accounted to Basidomycetes [1], which however accounted for less than 5 % of fungal protein in all analyzed samples. Among bacteria, lignin degradation was reported for Actinomycetes, α- , and γ-Proteobacteria [13]. The change in controls over lignin degradation after 6 months (i.e. lignin degradation dependent on litter stoichiometry) was accompanied by increased abundances of Actinomycetes and α-Proteobacteria while γ-Proteobacteria abundance was correlated to lignin degradation activity after 6 months of incubation. In contrast, several Ascomycetes classes (Sordariomycetes, Saccheromycetes), which were highly abundant in early decomposition stages and are associated with the rapid degradation of labile C substrates, decreased in their relative abundance. However, since the metaproteomic approach did not find relevant amounts of oxidative extracellular enzymes we so far cannot dissect the contributions of bacteria and fungi to the lignin decomposition process.

Conclusions

Our results contradict the traditional concept that lignin decomposition is slow during early litter decomposition. While traditional litter decomposition models propose that lignin decomposition mainly occurs during late decomposition stages, we found that variable but in some cases substantial amounts of lignin were decomposed during the first 6 months. We can therefore conclude, that low nutrient levels (mainly P) led to an earlier onset of lignin degradation (Q1). On the other hand, the results of our experiment

contradicted our second hypothesis (Q2): We found that regardless of their wider C:N and C:P ratios, fungal communities were more dominant in litter with high litter N and P contents, especially within the first 6 months of decomposition. Regardless of low F:B ratios, P-poor, but bacteria-rich communities were most actively degrading lignin during early decomposition. In contrast, late lignin decomposition rates were highest in N-rich litter with high F:B ratios, indicating a fundamental change in the controls of lignin decomposition between early and later decomposition stages.

Material and methods

Litter decomposition experiment

Beech litter was collected at four different sites in Austria (Achenkirch (AK), Klausenleopoldsdorf (KL), Ossiach (OS), and Schottenwald (SW); referred to as litter types) in October 2008. Litter was cut to pieces of approximately 0.25cm^2, homogenized, sterilized twice by γ-radiation (35 kGy, 7 days between irradiations) and inoculated (1.5% w/w) with a mixture of litter and soil to assure that all litter types share the same initial microbial community. From each type, four samples of litter were taken immediately after inoculation, dried and stored at room temperature. Batches of 60g litter (fresh weight) were incubated at 15 °C and 60% relative water content in mesocosms for 15 months. For each litter type 5 replicates were removed and analyzed after 14, 97, 181 and 475 days. A detailed description of the litter decomposition experiment was published by [25].

Bulk litter, extractable, and microbial biomass nutrient content

To calculate litter mass loss, litter dry mass content was measurement in 5 g litter (fresh weight) after 48 h at 80 °C. Dried litter was ball-milled for further chemical analysis. Litter C and N content was determined using an elemental analyzer (Leco CN2000, Leco Corp., St. Joseph, MI, USA). Litter phosphorus content was measured with ICP-AES (Vista-Pro, Varian, Darmstadt, Germany) after acid digestion [26]). To determine dissolved organic C, dissolved N and P, 1.8 g litter (fresh weight) were extracted with 50 ml 0.5 M K_2SO_4. Samples were shaken on a reciprocal shaker with the extractant for 30 minutes, filtered through ash-free cellulose filters and frozen at -20 °C until analysis. To quantify microbial biomass C, N and P, further samples were additionally extracted under the same conditions after chloroform fumigation for 24 h [27]. Microbial biomass was determined as the difference between fumigated and non-fumigated extractions .

C and N concentration in extracts were determined with a TOC/TN analyzer (TOC-VCPH and TNM, Schimadzu), P was determined photometrically as inorganig P after persulfate digestion [28].

Substrate to consumer stoichiometric imbalances $C{:}X_{imbal}$ were calculated as

$$C : X_{imbal} = \frac{C : X_{litter}}{C : X_{microbial}} \tag{1}$$

where X stand for the element N or P.

Microbial Respiration

Respiration was monitored weekly during the entire incubation in mesocosms removed after 6 month and on the last incubation day for all mesocosms using an infrared gas analyzer (IRGA, EGM4 with SRC1, PPSystems, USA). CO2 concentration was measured over 70 seconds and increase per second was calculated based on initial dry mass. Accumulated respiration after 6 month was calculated assuming linear transition between measurements, accumulated respiration after 15 month was estimated from respiration rates after 181 and 475 days.

Potential enzyme activities

Potential activities of β-1,4-cellobiosidase ("cellulase"), phenoloxidase and peroxidase were measured immediately after sampling. 1 g of litter (fresh weight) was suspended in sodium acetate buffer (pH 5.5) and ultrasonicated. To determine cellulase activity, 200 µl suspension were mixed with 25 nmol 4-methylumbelliferyl-β-D-cellobioside (dissolved in 50 µl of the same buffer) in black microtiter plates and incubated for 140 min in the dark. The amount of methylumbelliferyl (MUF) set free in by the enzymatic reaction was measured flourimetrically (Tecan Infinite M200, exitation at 365 nm, detection at 450 nm). To measure phenoloxidase and peroxidase activity litter suspension was mixed 1:1 with a solution of L-3,4-dihydroxyphenylalanin (DOPA) to a final concentration of 10 mM. Samples were incubated in microtiter plates for 20h to determine phenoloxidase activity. For peroxidase activity, 1 nmol of H_2O_2 was added before incubation. Absortion at 450 nm was measured before and after incubation. All enzyme activities were measured in three analytical replicates. The assay is described in detail in [29].

Pyrolysis-GC/MS

Pyrolysis-GC/MS was performed with a Pyroprobe 5250 pyrolysis system (CDS Analytical) coupled to a Thermo Trace gas chromatograph and a DSQ II MS detector (both Thermo Scientific) equipped with a carbowax colomn (Supelcowax 10, Sigma-Aldrich). Between 2-300 µg of dried and finely ground litter (MM2000 ball mill, Retsch) was heated to 600 °C for 10 seconds in a helium atmosphere. GC oven temperature was constant at 50 °C for 2 minutes, followed by an increase of 7 °C/min to a final temperature of 260 °C, which was held for 15 minutes. The MS detector was set for electron ionization at 70 eV in the scanning mode (m/z 20 to 300).

Peaks were assignment was based on NIST 05 MS library after comparison with measured reference materials. 128 peaks were identified and selected for integration either because of their abundance or diagnostic value. This included 28 lignin and 45 carbohydrate derived substances. The pyrolysis products used are stated in tables 2 -4 For each peak between one and four dominant and specific mass fragments were selected, integrated and converted to TIC peak areas by multiplication with a MS response coefficient [30, 31]. Peak areas are stated as % of the sum of all integrated peaks.

A pyrolysis-based lignin to carbohydrate index (LCI) was calculated to derive a ratio between these two substance classes without influences of changes in the abundance of other compounds .

$$LCI = \frac{Lignin}{Lignin + Carbohydrates} \tag{2}$$

Accounting for carbon loss, we estimate % lignin and cellulose degraded during decomposition according to equation 3, where $\%_{init}$ and $\%_{act}$ stand for initial and actual %TIC area of lignin or cellulose pyrolysis products, C_{init} for the initial amount of C and R_{acc} for the accumulated CO_2-C respired by a mesocosm.

$$\%_{loss} = 100 \cdot \frac{\%_{init} - \%_{act}}{\%_{init}} \cdot \frac{(1 - R_{acc})}{C_{init}} \tag{3}$$

Metaproteome analysis and quantitative PCR

From each harvest (14, 97, 181, and 475 days), one replicate per litter type was stored at -80°C for metaproteome analysis. 3 g of each sample were grounded in liquid nitrogen and extracted with Tris/KOH buffer (pH 7.0) containing 1% SDS. Samples were sonicated for 2 min, boiled for 20 min and shaken at 4 °C for 1 h. Extracts were centrifuged twice to remove debris and concentrated by vacuum-centrifugation. An aliquot of

the sample was applied to a 1D-SDS-PAGE and subjected to in-gel tryptic digestion. The resulting peptide mixtures were analyzed on a hybrid LTQ-Orbitrap MS (Thermo Fisher Scientific) as described earlier [32]. Protein database search against the UniRef 100 database, which also comprised the translated metagenome of the microbial community of a Mennesota farm silage soil [33] and known contaminants, was performed using the MASCOT Search Engine. A detailed description of the extraction procedure and search criteria was published by [34]. If more than one protein was identified based on the same set of spectra these proteins were grouped together resulting in one protein cluster. The obtained protein/protein cluster hits were assigned to phylogenetic and functional groups and assignments were validated by the PROPHANE workflow (http://prophane.svn.sourceforge.net/viewvc/prophane/trunk/; [35]). Higher protein abundance is represented by a higher number of MS/MS spectra acquired from peptides of the respective protein. Thus, protein abundances were calculated based on the normalised spectral abundance factor (NSAF) [36,37]. This number allows relative comparison of protein abundances over different samples [38]. Protein abundances was aggregated at class level for fungi and protebacteria and at phylum level for other bacterial taxa. These abundances were subjected to a canonical correspondance analysis without constrains. Vectorial fittings of stoichiometrical ratios (litter, microbial biomass and imbalance) were calculated and plotted when $p < 0.05$.

Quantitative PCR was used to determine fungal and bacterial abundance as described recently [39]. F:B ratios were calculated as the ratio between estimated amounts of bacterial and fungal DNA found.

Statistical analysis

All statistical analyses were performed with the software and statistical computing environment R [40]. If not mentioned otherwise, results were considered significant when $p < 0.05$. Due to frequent variance inhomogeneities Welch ANOVA and paired Welch's t-tests with Bonferroni corrected p limits were used. All correlations mentioned refer to Pearson correlations. A correspondence analysis (CA) and vectorial fittings were calculated using the R package "vegan" [41].

Acknowledgments

This study formed part of the national research network MICDIF (Linking microbial diversity and functions across scales and ecosystems, S-10007-B01, -B06 and -B07) by the Austrian Research Fund (FWF). Katharina Keiblinger is a recipient of a DOC-fFORTE fellowship of the Austrian Academy of Sciences. Vital support regarding Pyr-GC/MS measurments was given by Clemens Schwarzinger, Andreas Blöchl and Birgit Wild.

References

1. Berg, B & McClaugherty C (2008) Plant Litter. Decomposition, Humus Formation, Carbon Sequestration. Berlin: Springer.

2. Don A, Kalbitz K (2005) Amounts and degradability of dissolved organic carbon from foliar litter at different decomposition stages. Soil Biology and Biochemistry 37: 2171–2179.

3. Sinsabaugh RL (2010) Phenol oxidase, peroxidase and organic matter dynamics of soil. Soil Biology and Biochemistry 42: 391–404.

4. Berg B, Staaf H (1980) Decomposition rate and chemical changes of Scots pine needle litter. II. Influence of chemical composition. Ecological Bulletins : 373–390.

5. Coûteaux MM, Bottner P, Berg B (1995) Litter decomposition, climate and liter quality. Trends in ecology & evolution 10: 63–66.

6. Moorhead DL, Sinsabaugh RL (2006) A theoretical model of litter decay and microbial interaction. Ecological Monographs 76: 151–174.

7. Adair EC, Parton WJ, Del Grosso SJ, Silver WL, Harmon ME, et al. (2008) Simple three-pool model accurately describes patterns of long-term litter decomposition in diverse climates. Global Change Biology : 2636–2660.

8. Hatfield RD, Romualdo SF (2005) Can Lignin Be Accurately Measured? Crop Science 45: 832–839.

9. Preston CM, Trofymow JA, Sayer BG, Niu J (1997) 13C nuclear magnetic resonance spectroscopy with cross-polarization and magic-angle spinning investigation of the proximate analysis fractions used to assess litter quality in decomposition studies. Canadian Journal of Botany 75: 1601–1613.

10. Amelung W, Brodowski S, Sandhage-Hofmann A, Bol R (2008) Combining Biomarker with Stable Isotope Analyses for Assessing the Transformation and Turnover of Soil Organic Matter. Advances in Agronomy 100: 155–250.

11. Thevenot M, Dignac MF, Rumpel C (2010) Fate of lignins in soils: A review. Soil Biology and Biochemistry 42: 1200–1211.

12. Bol R, Poirier N, Balesdent J, Gleixner G (2009) Molecular turnover time of soil organic matter in particle - size fractions of an arable soil. Rapid Communications in Mass Spectrometry 23: 2551–2558.

13. Bugg TD, Ahmad M, Hardiman EM, Singh R (2011) The emerging role for bacteria in lignin degradation and bio-product formation. Current opinion in biotechnology 22: 394–400.

14. Klotzbücher T, Kaiser K, Guggenberger G, Gatzek C, Kalbitz K (2011) A new conceptual model for the fate of lignin in decomposing plant litter. America 92: 1052–1062.

15. Achyuthan KE, Achyuthan AM, Adams PD, Dirk SM, Harper JC, et al. (2010) Supramolecular self-assembled chaos: polyphenolic lignin's barrier to cost-effective lignocellulosic biofuels. Molecules (Basel, Switzerland) 15: 8641–88.

16. Dyckmans J, Flessa H, Brinkmann K, Mai C, Polle A (2002) Carbon and nitrogen dynamics in acid detergent fibre lignins of beech (Fagus sylvatica L.) during the growth phase. Plant, Cell & Environment 25: 469–478.

17. Craine JM, Morrow C, Fierer N (2007) Microbial nitrogen limitation increases decomposition. Ecology 88: 2105–13.

18. Knorr M, Frey S, Curtis P (2005) Nitrogen addition and litter decomposition : A meta-analysis. Ecology 86: 3252–3257.

19. Fontaine S, Henault C, Aamor a, Bdioui N, Bloor J, et al. (2011) Fungi mediate long term sequestration of carbon and nitrogen in soil through their priming effect. Soil Biology and Biochemistry 43: 86–96.

20. Talbot JM, Yelle DJ, Nowick J, Treseder KK (2011) Litter decay rates are determined by lignin chemistry. Biogeochemistry : 1–17–17.

21. Mooshammer M, Wanek W, Schnecker J, Wild B, Leitner S, et al. (2011) Stoichiometric controls of nitrogen and phosphorus cycling in decomposing beech leaf litter. Ecology in press.

22. Sterner RW, Elser JJ (2002) Ecological Stoichiometry.

23. Leitner S, Wanek W, Wild B, Haemmerle I, Kohl L, et al. (2011) Linking resource quality to decomposition processes: Influence iof litter chemistry and stoichiometry on glucan depolymerization during decomposition of beech (Fagus silvatica L.) litter. Soil Biology and Biochemistry in review.

24. Janshekar H, Fiechter A (1988) Cultivation of Phanerochaete chrysosporium and production of lignin peroxidases in submerged stirred tank reactors. Journal of Biotechnology 8: 97–112.

25. Wanek W, Mooshammer M, Blöchl A, Hanreich A, Keiblinger K, et al. (2010) Determination of gross rates of amino acid production and immobilization in decomposing leaf litter by a novel N-15 isotope pool dilution technique. Soil Biology and Biochemistry 42: 1293–1302.

26. Kolmer J, Spaulding E, Robinson H (1951) Approved Laboratory Techniques. New York: Appleton Century Crafts.

27. Brooks P, Kragt J, Powlson D, Jenkinson D (1985) Chloroform fumigation and the release of soil nitrogen: the effects of fumigation time and temperature. Soil Biology & Biochemistry 17: 831–835.

28. Schinner F, Öhlinger R, Kandeler E, Margesin R (1996) Methods in Soil Biology. Berlin: Springer Verlag, pp. 389 pp.

29. Kaiser C, Koranda M, Kitzler B, Fuchslueger L, Schnecker J, et al. (2010) Belowground carbon allocation by trees drives seasonal patterns of extracellular enzyme activities by altering microbial community composition in a beech forest soil. New Phytologist 187: 843–858.

30. Schellekens J, Buurman P, Pontevedra-Pombal X (2009) Selecting parameters for the environmental interpretation of peat molecular chemistry - A pyrolysis-GC/MS study. Organic Geochemistry 40: 678–691.

31. Kuder T, Kruge MA (1998) Preservation of biomolecules in sub-fossil plants from raised peat bogs - a potential paleoenvironmental proxy. Organic Geochemistry 29: 1355–1368.

32. Schneider T, Gerrits B, Gassmann R, Schmid E, Gessner MO, et al. (2010) Proteome analysis of fungal and bacterial involvement in leaf litter decomposition. Proteomics 10: 1819–30.

33. Tringe SG, von Mering C, Kobayashi A, Salamov Aa, Chen K, et al. (2005) Comparative metagenomics of microbial communities. Science (New York, NY) 308: 554–7.

34. Keiblinger KM, Schneider T, Roschitzki B, Schmid E, Eberl L, et al. (2011) Effects of stoichiometry and temperature perturbations on beech litter decomposition, enzyme activities and protein expression. Biogeosciences Discussions 8: 11827–11861.

35. Schneider T, Schmid E, de Castro JaV, Cardinale M, Eberl L, et al. (2011) Structure and function of the symbiosis partners of the lung lichen (Lobaria pulmonaria L. Hoffm.) analyzed by metaproteomics. Proteomics : 2752–2756.

474 36. Florens L, Carozza MJ, Swanson SK, Fournier M, Coleman MK, et al. (2006) Analyzing chromatin
475 remodeling complexes using shotgun proteomics and normalized spectral abundance factors. Methods
476 (San Diego, Calif) 40: 303–11.

477 37. Zybailov B, Mosley AL, Sardiu ME, Coleman MK, Florens L, et al. (2006) Statistical analysis of
478 membrane proteome expression changes in Saccharomyces cerevisiae. Journal of proteome research 5:
479 2339–47.

480 38. Bantscheff M, Schirle M, Sweetman G, Rick J, Kuster B (2007) Quantitative mass spectrometry in
481 proteomics: a critical review. Analytical and bioanalytical chemistry 389: 1017–31.

482 39. Inselsbacher E, Hinko-Najera Umana N, Stange FC, Gorfer M, Schüller E, et al. (2010) Short-term
483 competition between crop plants and soil microbes for inorganic N fertilizer. Soil Biology and Bio-
484 chemistry 42: 360–372.

485 40. R Development Core Team (2008). R: A Language and Environment for Statistical Computing. URL
486 `http://www.r-project.org`.

487 41. Oksanen J, Blanchet FG, Kindt R, Legendre P, O'Hara R, et al. (2011). vegan: Community Ecology
488 Package. R packge version 1.17-9. URL `http://cran.r-project.org/package=vegan`.

Figure Legends

Figure 1. Respiration rates, concentration of soluble organic C and potential extracellular enzyme activities in decomposing beech leaf litter from a mesocosm experiment. Beech litter was collected in: triangles, Schottenwald (SW); diamonds, Ossiach (OS); squares, Klausenleopoldsdorf (KL); circles, Achenkirch, AK. Error bars indicate standard errors (n=5). Significant differences between litter types are presented by asterisks above the symbols, significant differences between time points by asterisks to the right of the curves. *, $P<0.05$, **, $P<0.01$, ***, $P<0.001$, b.d. - below detection limit.

Figure 2. Microbial biomass C, N and P, microbial C:N:P stoichiometry and resource:consumer stoichiometric imbalance in these elements in decomposing beech leaf litter from a mesocosm experiment. Beech litter was collected in: triangles, Schottenwald (SW); diamonds, Ossiach (OS); squares, Klausenleopoldsdorf (KL); circles, Achenkirch, AK. Error bars indicate standard errors (n=5). Significant differences between litter types are presented by asterisks above the symbols, significant differences between time points by asterisks to the right of the curves. *, $P<0.05$, **, $P<0.01$, ***, $P<0.001$.

Figure 3. Protein abundance of fungal and bacterial taxa. Litter was collected in Achenkirch (AK);, Klausenleopoldsdorf (KL); Ossiach (OS); Schottenwald (SW). Samples were analyzed after sterilization, re-innoculation and incubation for 14, 97, 181, or 475 days.

Figure 4. Fungi:Bacteria (F:B) ratios and their correlations with LCI change: A: F:B protein abundance (left) and DNA (right) ratio. B: Correlations between F:B preotein abundance ratios and lignin loss (top), carbohydrate loss (mid) and lignin loss : carbon loss (bottom) for 0-6 months (left) and 6-15 months (right, errorbars indicate standard errors, n=4-5). Beech litter was collected in: triangles, Schottenwald (SW); diamonds, Ossiach (OS); squares, Klausenleopoldsdorf (KL); circles, Achenkirch, AK. Error bars indicate standard errors (n=5). Significant differences between litter types are presented by asterisks above the symbols, significant differences between time points by asterisks to the right of the curves. *, $P<0.05$, **, $P<0.01$, ***, $P<0.001$.

Figure 5. Develoment of lignin to carbohydrate index (lignin : (lignin+carbohydrates), LCI) during time of beech litter decomposition (left) or plotted against cumulative C loss (right). Errorbars indicate standard errors (n=4-5). The dashed line indicates a constant ratio between lignin and carbohydrates (i.e. no preferential decomposition of carbohydrates. Beech litter was collected in: triangles, Schottenwald (SW); diamonds, Ossiach (OS); squares, Klausenleopoldsdorf (KL); circles, Achenkirch, AK. Error bars indicate standard errors (n=5). Significant differences between litter types are presented by asterisks above the symbols, significant differences between time points by asterisks to the right of the curves. *, $P<0.05$, **, $P<0.01$, ***, $P<0.001$.

Figure 6. Carbon loss corrected amounts of lignin and carbohydrates degraded in beech litter collected in Achenkirch (AK), Klausenleopoldsdorf (KL), Ossiach (OS) and Schottenwald (SW). Carbon loss was calculated based on accumulated respiration for each mesocosm. Error bars indicate standard errors (n=4-5). The dashed line marks no discrimation during decomposition between lignin, carbohydrates and bulk carbon

Figure 7. Correlation between the LCI change or the ratio of lignin : carbohydrate decomposition ratio during the first 6 months of litter decomposition correlate to litter : microbe stoichiometric imbalances. and change and Correlations between lignin accumulation during the first 6 month of litter incubation and stoichiometric resource:consumer imbalances. LCI is calculates as of lignin/(lignin+Carbohydrates). Beech litter was collected in: triangles, Schottenwald (SW); diamonds, Ossiach (OS); squares, Klausenleopoldsdorf (KL); circles, Achenkirch, AK. *, $P<0.05$, **, $P<0.01$, ***, $P<0.001$.

Figure 8. Microbial commuity composition. The first two components of a correspondance analysis (CA) of protein abundances found. Rectangles indicate samples of identical incubation time. Peptides were aggregated at class level (fungi and proteobacteria) or phylum level (other bacterial phyla): Dothideomycetes (Doth); Eurotiomycetes (Euro); Leotiomycetes (Leot); Saccharomycetes (Sacc); Sordariomycetes (Sord); Agaricomycetes (Agar); Tremellomycetes (Trem); Ustilaginomycetes (Usti); Thermotogae (Ther); Bacteroidetes (Bact); Actinobacteria (Acti); Cyanobacteria (Cyan); Firmicutes (Firm); Fusobacteria (Fuso); Verrucomicrobia (Verr); Dictyoglomi (Dict); Alphaproteobacteria (Alph); Betaproteobacteria (Beta); Gammaproteobacteria (Gamm); Deltaproteobacteria (Delt); Epsilonproteobacteria (Epsi). Taxa factor loadings were printed x2 for better readability. Correlations between CA 1, CA 2, and litter chemistry, microbial stoichiometry, and protein abundance of microbial taxa are stated in supplemental table **??**. Arrows represent vectorial fittings of these variables calculated independently from the CA, plotted only if $p<0.05$: Litter C content (C lit); $C:X_{Microbial}/C:X_{Litter}$ (C:P imb, C:N imb).

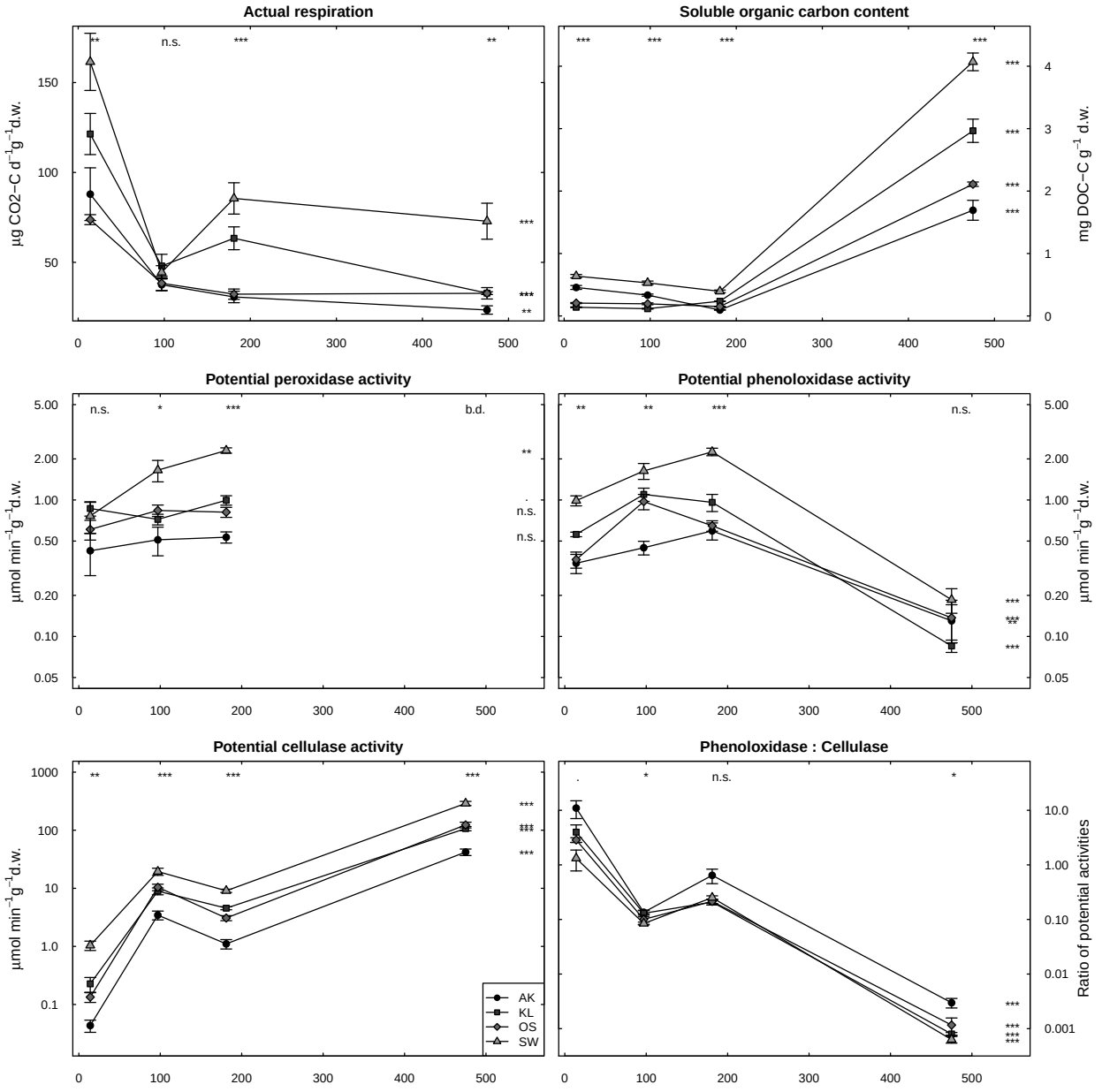

Figure 9. Respiration rates, concentration of soluble organic C and potential extracellular enzyme activities in decomposing beech leaf litter from a mesocosm experiment. Beech litter was collected in: triangles, Schottenwald (SW); diamonds, Ossiach (OS); squares, Klaus-nleopoldsdorf (KL); circles, Achenkirch, AK. Error bars indicate standard errors (n=5). Significant differences between litter types are presented by asterisks above the symbols, significant differences between time points by asterisks to the right of the curves. *, P<0.05, **, P<0.01, ***, P<0.001, b.d. - below detection limit.

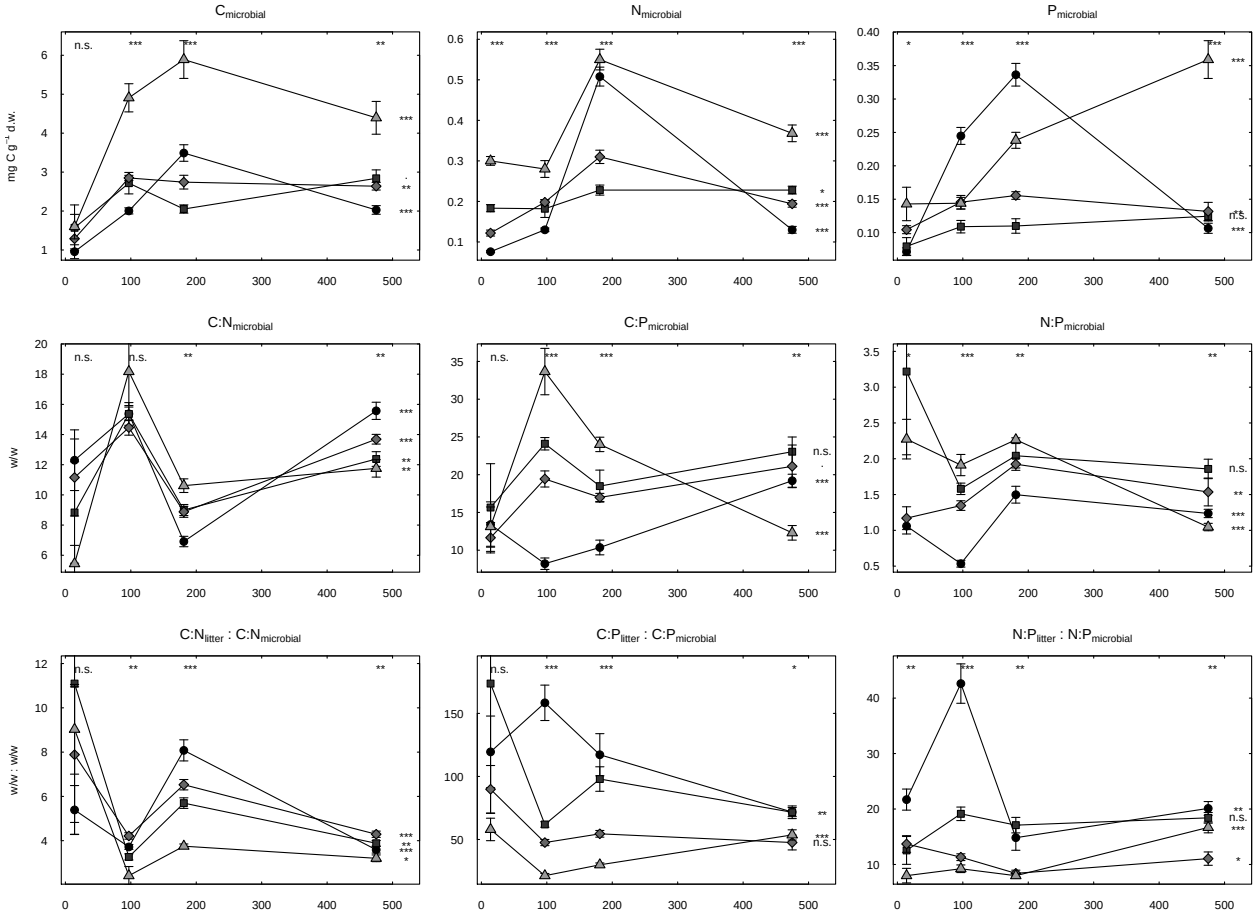

Figure 10. Microbial biomass C, N and P, microbial C:N:P stoichiometry and resource:consumer stoichiometric imbalance in these elements in decomposing beech leaf litter from a mesocosm experiment. Beech litter was collected in: triangles, Schottenwald (SW); diamonds, Ossiach (OS); squares, Klausenleopoldsdorf (KL); circles, Achenkirch, AK. Error bars indicate standard errors (n=5). Significant differences between litter types are presented by asterisks above the symbols, significant differences between time points by asterisks to the right of the curves. *, $P<0.05$, **, $P<0.01$, ***, $P<0.001$.

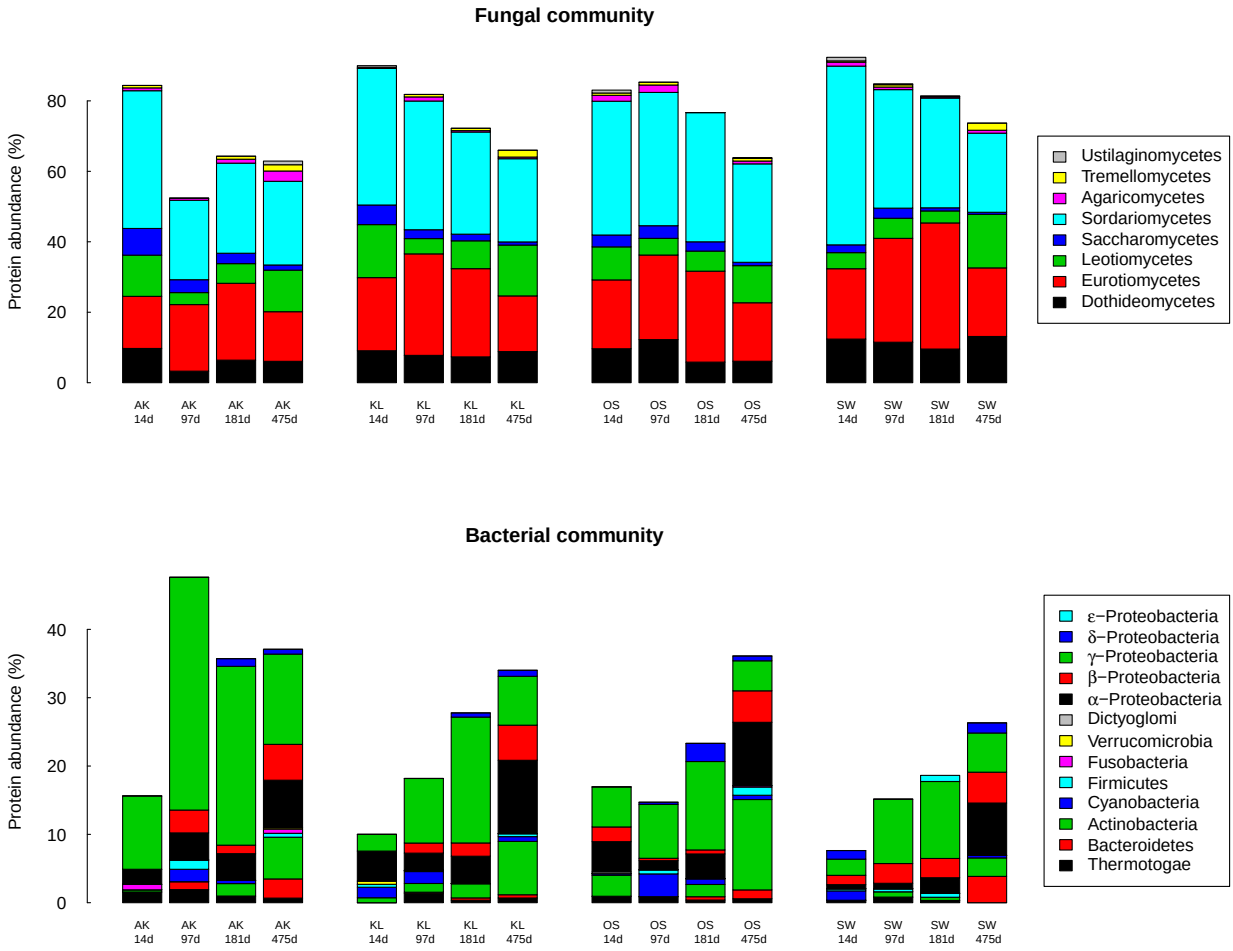

Figure 11. Protein abundance of fungal and bacterial taxa. Litter was collected in Achenkirch (AK);, Klausenleopoldsdorf (KL); Ossiach (OS); Schottenwald (SW). Samples were analyzed after sterilization, re-innoculation and incubation for 14, 97, 181, or 475 days.

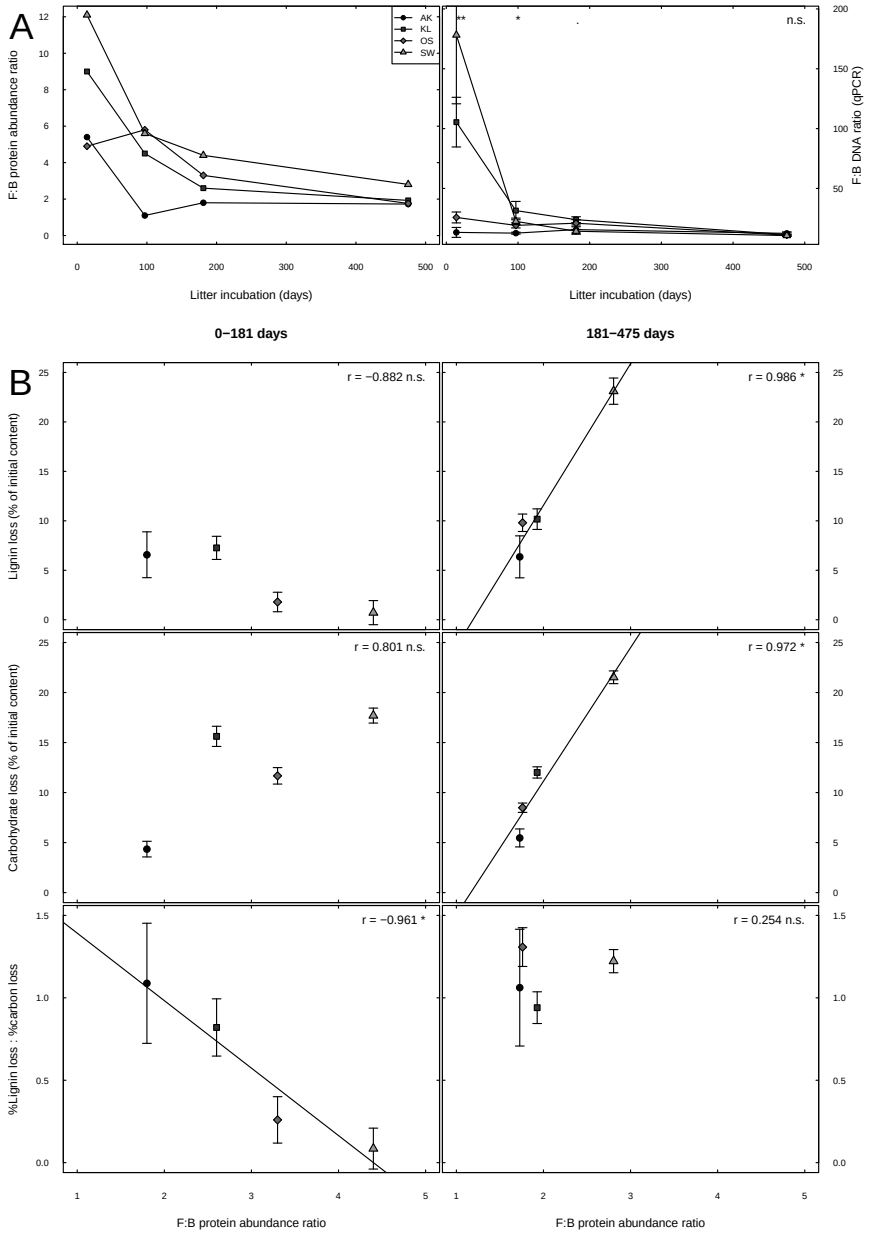

Figure 12. Fungi:Bacteria (F:B) ratios and their correlations with LCI change: A: F:B protein abundance (left) and DNA (right) ratio. B: Correlations between F:B preotein abundance ratios and lignin loss (top), carbohydrate loss (mid) and lignin loss : carbon loss (bottom) for 0-6 months (left) and 6-15 months (right, errorbars indicate standard errors, n=4-5). Beech litter was collected in: triangles, Schottenwald (SW); diamonds, Ossiach (OS); squares, Klausenleopoldsdorf (KL); circles, Achenkirch, AK. Error bars indicate standard errors (n=5). Significant differences between litter types are presented by asterisks above the symbols, significant differences between time points by asterisks to the right of the curves. *, $P<0.05$, **, $P<0.01$, ***, $P<0.001$.

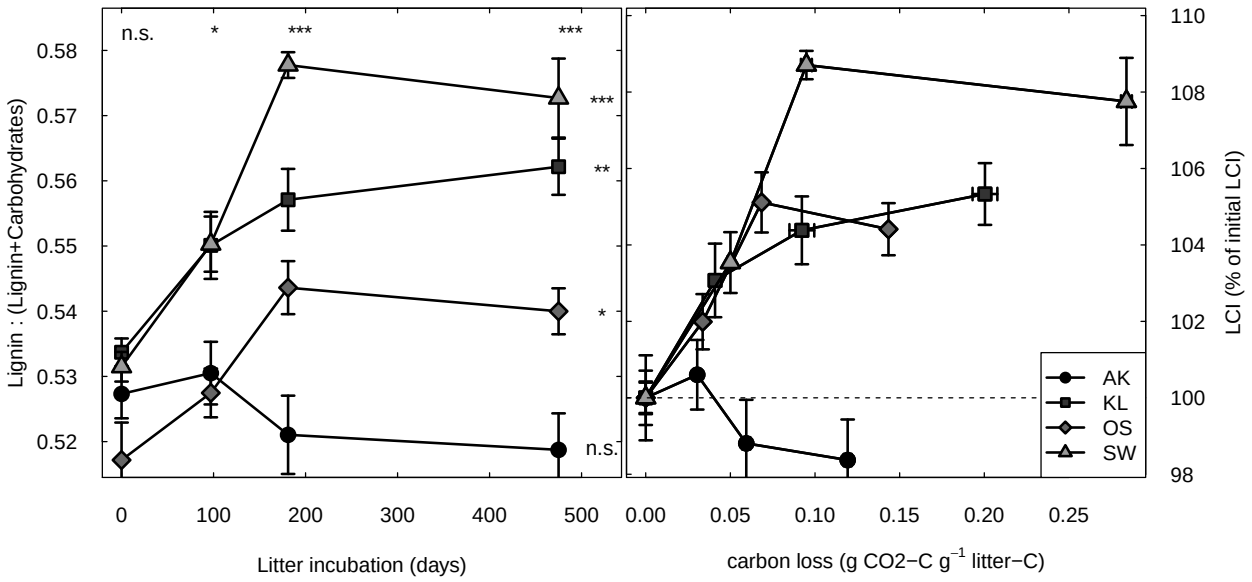

Figure 13. Develoment of lignin to carbohydrate index (lignin : (lignin+carbohydrates), LCI) during time of beech litter decomposition (left) or plotted against cumulative C loss (right). Errorbars indicate standard errors (n=4-5). The dashed line indicates a constant ratio between lignin and carbohydrates (i.e. no preferential decomposition of carbohydrates. Beech litter was collected in: triangles, Schottenwald (SW); diamonds, Ossiach (OS); squares, Klausenleopoldsdorf (KL); circles, Achenkirch, AK. Error bars indicate standard errors (n=5). Significant differences between litter types are presented by asterisks above the symbols, significant differences between time points by asterisks to the right of the curves. *, $P<0.05$, **, $P<0.01$, ***, $P<0.001$.

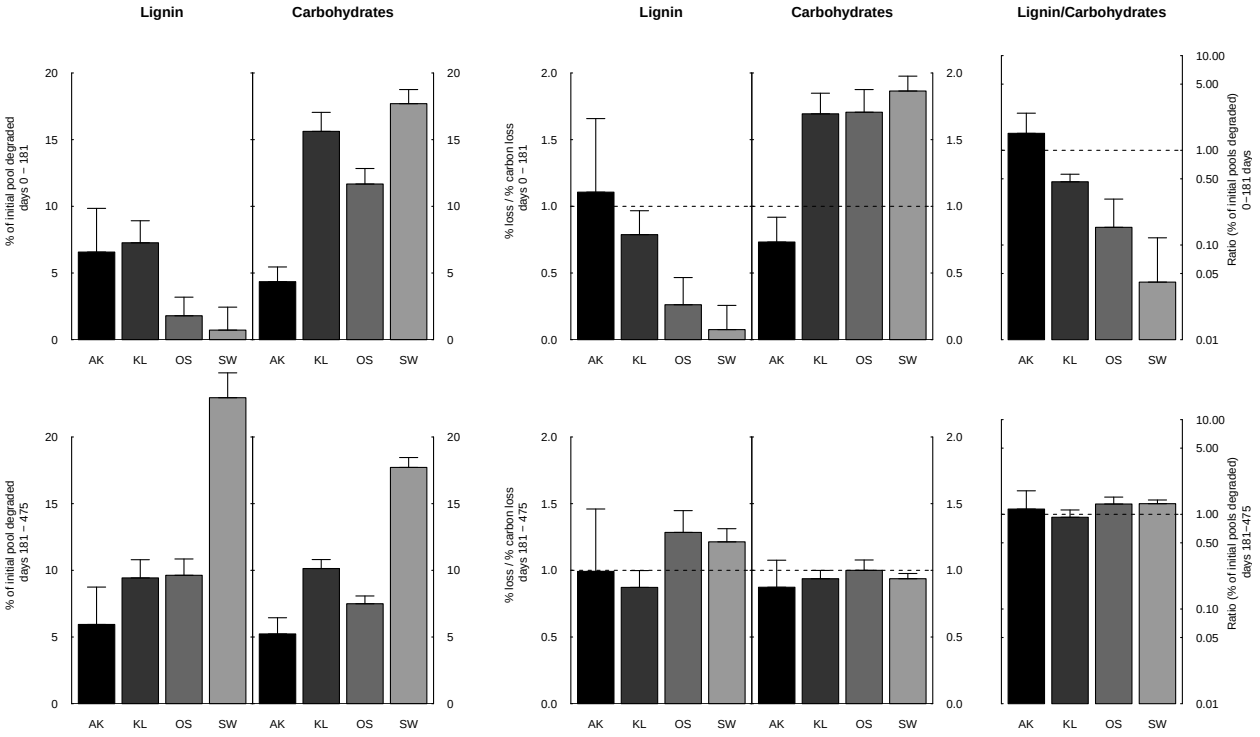

Figure 14. Carbon loss corrected amounts of lignin and carbohydrates degraded in beech litter collected in Achenkirch (AK), Klausenleopoldsdorf (KL), Ossiach (OS) and Schottenwald (SW). Carbon loss was calculated based on accumulated respiration for each mesocosm. Error bars indicate standard errors (n=4-5). The dashed line marks no discrimation during decomposition between lignin, carbohydrates and bulk carbon

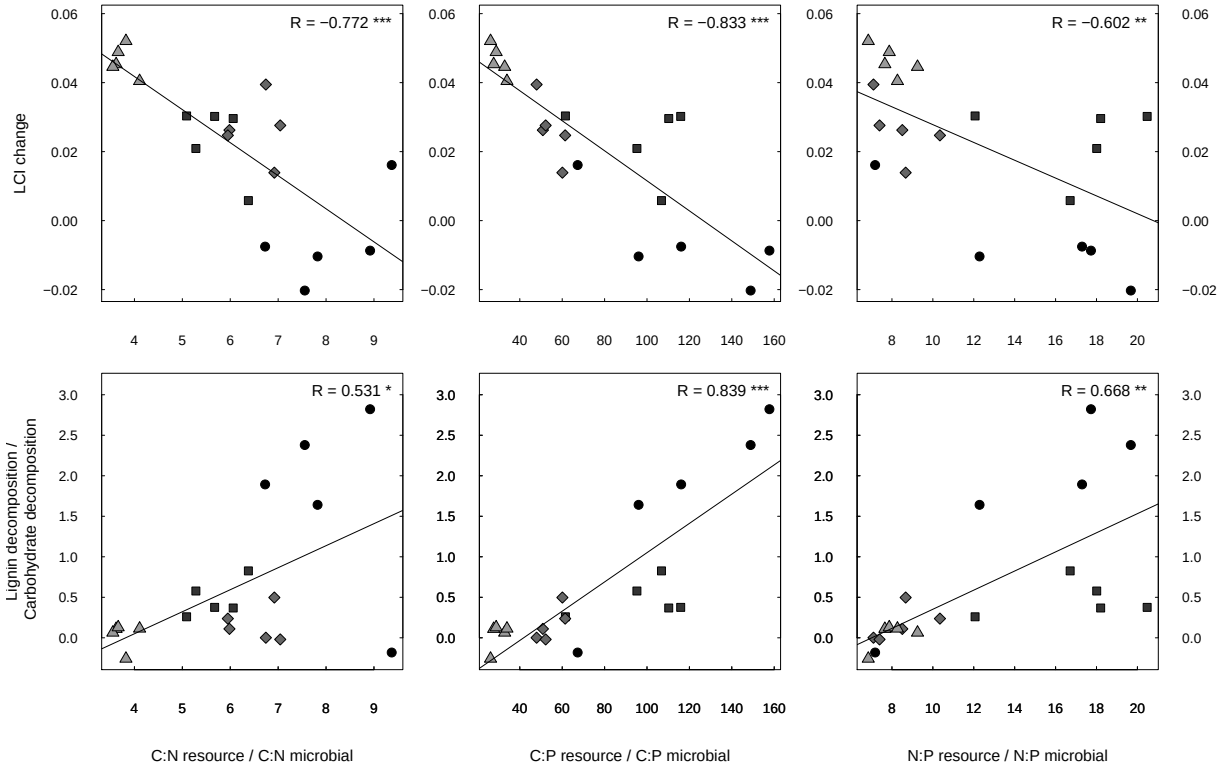

Figure 15. Correlation between the LCI change or the ratio of lignin : carbohydrate decomposition ratio during the first 6 months of litter decomposition correlate to litter : microbe stoichiometric imbalances. and change and Correlations between lignin accumulation during the first 6 month of litter incubation and stoichiometric resource:consumer imbalances. LCI is calculates as of lignin/(lignin+Carbohydrates). Beech litter was collected in: triangles, Schottenwald (SW); diamonds, Ossiach (OS); squares, Klausenleopoldsdorf (KL); circles, Achenkirch, AK. *, P<0.05, **, P<0.01, ***, P<0.001.

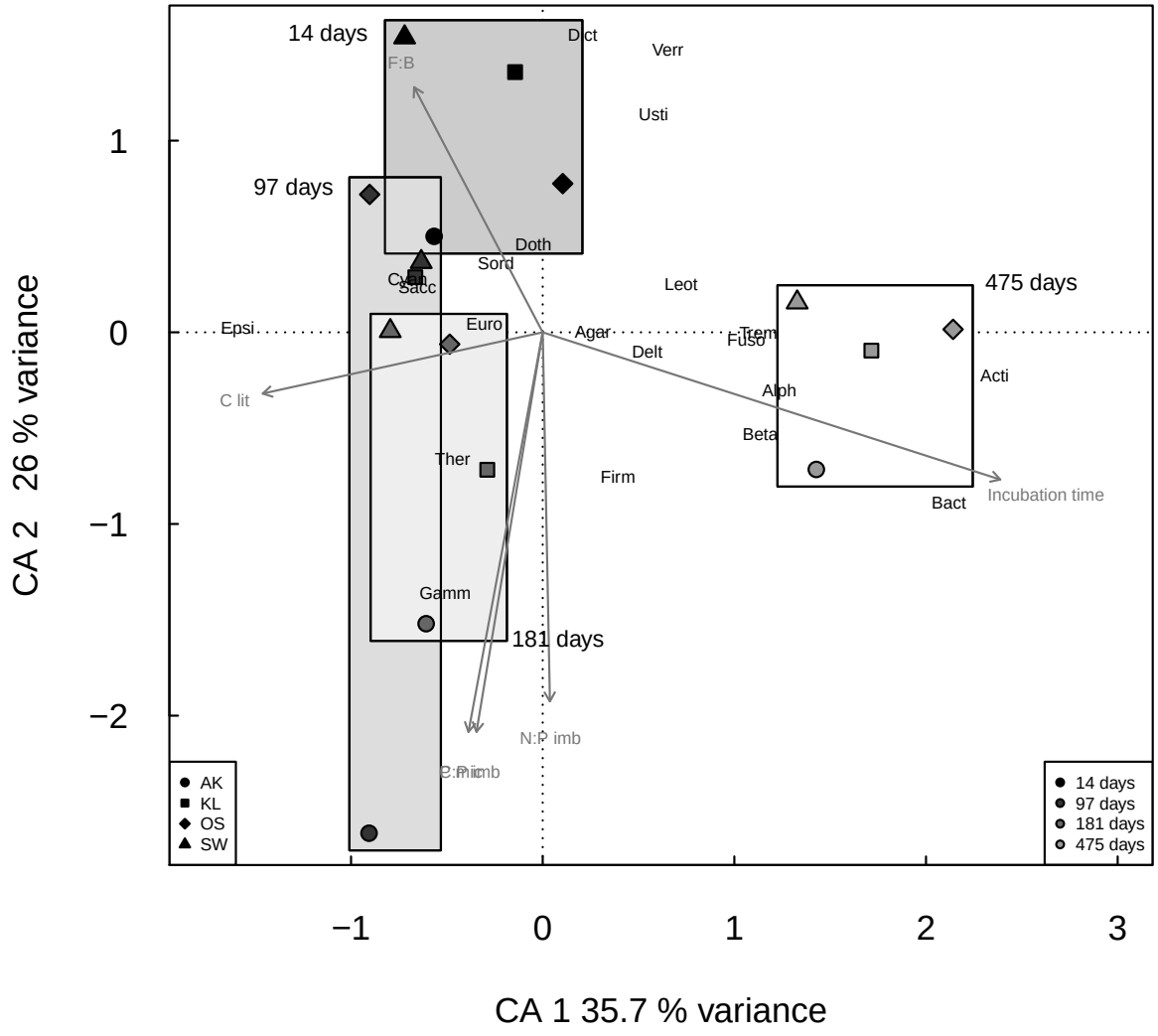

Figure 16. Microbial commuity composition. The first two components of a correspondance analysis (CA) of protein abundances found. Rectangles indicate samples of identical incubation time. Peptides were aggregated at class level (fungi and proteobacteria) or phylum level (other bacterial phyla): Dothideomycetes (Doth); Eurotiomycetes (Euro); Leotiomycetes (Leot); Saccharomycetes (Sacc); Sordariomycetes (Sord); Agaricomycetes (Agar); Tremellomycetes (Trem); Ustilaginomycetes (Usti); Thermotogae (Ther); Bacteroidetes (Bact); Actinobacteria (Acti); Cyanobacteria (Cyan); Firmicutes (Firm); Fusobacteria (Fuso); Verrucomicrobia (Verr); Dictyoglomi (Dict); Alphaproteobacteria (Alph); Betaproteobacteria (Beta); Gammaproteobacteria (Gamm); Deltaproteobacteria (Delt); Epsilonproteobacteria (Epsi). Taxa factor loadings were printed x2 for better readability. Correlations between CA 1, CA 2, and litter chemistry, microbial stoichiometry, and protein abundance of microbial taxa are stated in supplemental table **??**. Arrows represent vectorial fittings of these variables calculated independently from the CA, plotted only if $p<0.05$: Litter C content (C lit); $C{:}X_{Microbial}/C{:}X_{Litter}$ (C:P imb, C:N imb).

Table 1. Element concentrations, elemental stoichiometry and cellulose and lignin concentrations in beech litter measured after 14 days incubation. Standard errors are given in brackets (n=5). C extr represents for soluble organic carbon. Beech litter was collected in AK, Achenkirch, KL, Klausenleopoldsdorf, OS, Ossiach, and SW, Schottenwald.

	AK	(SE)	KL	(SE)	OS	(SE)	SW	(SE)	p value
C (% d.w.)	50.86	(0.39)	49.41	(0.53)	48.15	(0.39)	48.90	(0.34)	0.002
C extr (mg g-1)	0.46	(0.03)	0.14	(0.01)	0.21	(0.01)	0.64	(0.03)	<0.001
N (% d.w.)	0.878	(0.012)	0.938	(0.012)	0.806	(0.013)	1.172	(0.016)	<0.001
P (% d.w.)	0.040	(0.000)	0.030	(0.000)	0.052	(0.002)	0.070	(0.000)	<0.001
C:N (w/w)	57.86	(0.57)	52.60	(0.49)	59.97	(0.72)	41.78	(0.76)	<0.001
C:P (w/w)	1282	(21)	1548	(25)	905	(15)	699	(9)	<0.001
N:P (w/w)	22.17	(0.47)	29.45	(0.60)	15.10	(0.29)	16.75	(0.39)	<0.001
K (mg g-1)	0.26	(0.00)	0.54	(0.00)	0.21	(0.00)	0.55	(0.00)	<0.001
Ca (mg g-1)	1.33	(0.01)	1.26	(0.01)	1.63	(0.01)	1.23	(0.01)	<0.001
Mg (mg g-1)	0.27	(0.00)	0.14	(0.00)	0.20	(0.00)	0.15	(0.00)	<0.001
Fe (ppm)	210	(2)	208	(4)	453	(12)	192	(4)	<0.001
Mn (ppm)	172	(2)	1430	(10)	776	(9)	2137	(51)	<0.001
Zn (ppm)	30.8	(0.4)	33.0	(0.3)	36.0	(1.0)	42.4	(0.7)	<0.001
Lignin	28.9	(28.9)	29.9	(29.9)	31.2	(31.2)	30.5	(30.5)	<0.001
Carbohydrates	25.9	(25.9)	26.1	(26.1)	29.2	(29.2)	26.9	(26.9)	<0.001

Table 2. Lignin derived and other phenolic pyrolysis products

Name	RT	MW	integrated frements	Origin	Class
Guaiacol	18.87	124	109+124	Lignin	Guaiacyl
Methylguaiacol	20.32	138	123+138	Lignin	Guaiacyl
Ethylguaiacol	21.40	152	137+152	Lignin	Guaiacyl
Propenylguaiacol	23.29	164	149+164	Lignin	Guaiacyl
Vinylguaiacol	23.69	150	135+150	Lignin	Guaiacyl
Propenylguaiacol	24.48	164	149+164	Lignin	Guaiacyl
Syringol	24.58	154	139+154	Lignin	Syringyl
Propenylguaiacol	25.66	164	149+164	Lignin	Guaiacyl
Methylsyringol	25.67	168	153+168	Lignin	Syringyl
Ethylsysringol	26.39	182	167+182	Lignin	Syringyl
Propenylsyringol	27.97	194	179+194	Lignin	Syringyl
Vinylsyringol	28.37	180	165+180	Lignin	Syringyl
Guaiacolaldehyde	28.40	152	109+152	Lignin	Guaiacyl
Propylguaiacol	28.72	166	137+166	Lignin	Guaiacyl
Oxo-hydroxy-etylguaiacol	28.77	182	182	Lignin	Guaiacyl
Propenylsyringol	28.91	194	179+194	Lignin	Syringyl
Oxo-ethylguaiacol	29.20	166	151+166	Lignin	Guaiacyl
Oxo-propylguaiacol	29.36	180	137+180	Lignin	Guaiacyl
Propenylsyringol	30.16	194	194+179	Lignin	Syringyl
Syringolaldehyde	32.68	182	139+182	Lignin	Syringyl
Oxo-hydroxy-ethylsyringol	32.80	212	212	Lignin	Syringyl
Guaiacolacetic acid	32.88	182	137+182	Lignin	Guaiacyl
Propylsyringol	33.15	196	181+196	Lignin	Syringyl
Oxo-propylsyringol	33.32	210	167+210	Lignin	Syringyl
Oxopropenylguaiacol	35.30	178	135+178	Lignin	Guaiacyl
Hydroxypropenylguaiacol	37.10	180	137+180	Lignin	Guaiacyl
Syringolacetic acid	38.78	212	212	Lignin	Syringyl
Oxo-propenylsyringol	43.06	208	165+208	Lignin	Syringyl
Phenol	21.02	94	65+66+94	Phenolic	
4-Methylphenol	22.11	108	107+108	Phenolic	
3-Methylphenol	22.22	108	107+108	Phenolic	
Ethylphenol	23.38	122	107+122	Phenolic	
Propenylphenol	26.93	134	133+134	Phenolic	
Propenylphenol	27.76	134	133+134	Phenolic	
Propylphenol	31.11	136	151+166	Phenolic	
Butylphenol	31.86	150	107+150	Phenolic	
4-Hydroxybenzaldehyde	32.70	122	121+122	Phenolic	
Hydroquinone	33.40	110	81+110	Phenolic	

Table 3. Carbohydrate derived pyrolysis products

Name	RT	MW	integrated framents	Origin	Class
Acetaldehyde	2.06	44	29+44	Carbohydrates	
Furan	2.35	68	39+68	Carbohydrates	Furan
Methylfuran	2.74	82	81+82	Carbohydrates	Furan
Methylfuran	2.91	82	81+82	Carbohydrates	Furan
Dimethylfuran	3.43	96	95+96	Carbohydrates	Furan
Dimethylfuran	3.66	96	95+96	Carbohydrates	Furan
Vinylfuran	5.01	94	65+94	Carbohydrates	Furan
Unknown furan	6.36	108	107+108	Carbohydrates	Furan
Cyclopentanone	6.99	105	84+105	Carbohydrates	Cyclopentenone
Methylfuran	7.62	82	53+82+83	Carbohydrates	Furan
2-Oxopropanoic acid, methylester	7.92	102	43+102	Carbohydrates	
1-Hydroxypropanone	9.24	74	43	Carbohydrates	
2-Cyclopenten-1-one	10.26	82	53+54+52	Carbohydrates	Cyclopentenone
2-Methyl-2-cyclopenten-1-one	10.51	96	53+96	Carbohydrates	Cyclopentenone
1-Hydroxy-2-propanone	10.69	88	57+88	Carbohydrates	Cyclopentenone
Unknown	11.38	unk	65+66+94	Carbohydrates	
3-Furaldehyd	11.57	96	95+96	Carbohydrates	Furan
2(5H)Furanon	11.69	98	55+98	Carbohydrates	Furan
Propanoic acid, methylester	12.10	102	43+102	Carbohydrates	
2-Furaldehyd	12.22	96	95+96	Carbohydrates	Furan
Acetylfuran	12.99	110	95+110	Carbohydrates	Cyclopentenone
3-Methyl-cyclopentanone	13.31	96	67+96	Carbohydrates	Cyclopentenone
Dimethylcyclopentenone	13.69	110	67+95+110	Carbohydrates	Cyclopentenone
5-Methyl-2-furancarboxaldehyde	14.23	110	109+110	Carbohydrates	Furan
2-Cyclopenten-1,4-dione	14.44	96	54+68+96	Carbohydrates	Cyclopentenone
Butyrolactone	15.22	86	56+86	Carbohydrates	
Unknown	15.56			Carbohydrates	
Furanmethanol	15.61	98	98	Carbohydrates	Cyclopentenone
5-Methyl-2(5H)-furanone	16.06	98	55+98	Carbohydrates	Furan
Unknown	16.17	unk	110	Carbohydrates	
1,2-Cylopentandione	17.51	98	55+98	Carbohydrates	Cyclopentenone
Unknown	17.67	unk	42+70	Carbohydrates	
2-Hydroxy-3-methyl-2-cyclopenten-1-one	18.14	98	98	Carbohydrates	Cyclopentenone
3-Methy-l1,2-cyclopentanedione	18.42	112	69+112	Carbohydrates	Cyclopentenone
Unknown	19.06		58+86+114	Carbohydrates	
Unknown	19.35		98+126	Carbohydrates	
Unknown	21.77		116	Carbohydrates	
Unknown	22.33		44	Carbohydrates	
Unknown	26.18		57+69	Carbohydrates	
5-Hydroxymethylfuran-1-carboxaldehyde	27.51	126	97+126	Carbohydrates	Furan
Unknown	31.67		73+135	Carbohydrates	
Laevoglucosan	40.44	172	60+73	Carbohydrates	

Table 4. Other pyrolysis products

Name	RT	MW	integrated framents	Origin	Class
25:0 Alkan	27.74	352	57+71	aliphatic	Alkan
25:1 Alken	28.34	350	57+69	aliphatic	Alken
27:0 Alkan	30.04	380	57+67	aliphatic	Alkan
27:1 Alken	30.63	378	57+65	aliphatic	Alken
29:0 Alkan	32.20	408	57+63	aliphatic	Alkan
29:1 Alken	32.82	406	57+61	aliphatic	Alken
Myristic acid (14:0)	2.35	68	39+68	Lipid	Fatty Acid
Palmitic acid (16:0)	2.74	82	81+82	Lipid	Fatty Acid
Stearuc acid (18:0)	2.91	82	81+82	Lipid	Fatty Acid
N-methyl-pyrrol	6.15	81	80+81	Protein	Pyrrol
Pyridine	6.90	95	52+79+95	Protein	Pyridine
Methylpyridine	7.50	93	66+92+93	Protein	Pyridine
Methylpyridine	7.54	93	66+92+93	Protein	Pyridine
methylpyridine	9.02	93	66+93	Protein	Pyridine
Pyrrol	13.11	67	39+41+67	Protein	Pyrrol
Methylpyrrol	13.81	81	80+81	Protein	Pyrrol
Methylpyrrol	14.10	81	80+81	Protein	Pyrrol
3-Hydroxypyridine	26.52	95	67+95	Protein	Pyridine
Indole	26.85	117	89+117	Protein	Indole
Methylindole	27.42	131	130+131	Protein	Indole
Toluene	4.54	92	91+92		Aromatic
Xylene	5.94	106	91+105+106		Aromatic
Xylene	6.09	106	91+105+106		Aromatic
Xylene	6.20	106	91+105+106		Aromatic
Xylene	6.99	105?	84+105?		Aromatic
Methoxytoluene	11.78	122	121+122		Aromatic
Indene	12.64	116	115+116		Aromatic
Benzaldehyde	13.35	106	77+106		Aromatic
Dihydrobenzofuran	26.19	120	91+119+120		Aromatic
Limonene	7.22	136	93		Terpene
Phytol	20.00	276	95+123	Chlorophyll	Terpene
Unknown aliphatic	22.82		58+71		aliphatic
Aceton	2.46	58	43		
2-Propenal	2.60	56	55+56		
Methanol	2.88	32	29+31+32		
3-Buten-2-one	3.39	70	55+70		
2,3-Butandione	3.67	86	69+86		
3-Penten-2-one	3.89	86	69+86		
2-Butanal	4.56	70	69+70		
2,3-Pentadione	4.77	100	57+100		
Hexanal	5.16	82	56+72+82		
1-Penten-3-one	11.28	84	55+84		
Hexan-2,4-dion	23.92	114	56+84+114		
unknown	15.98		119+134		
Unknown	20.85		81		
Unknown	20.86		82+95		
Unknown	22.43		98+128		
Unknown	27.76		138		